Unveiling of the SST gradient over the South China Sea and its possible relationship to the Asian precipitation

Unveiling of the SST gradient over the South China Sea and its possible relationship to the Asian precipitation

B H Vaid
School of Marine Sciences, Nanjing University of Information Science and Technology (NUIST), Nanjing, China.

bakshi32@gmail.com

Abstract. The present study examines the Sea Surface Temperature (SST) variations over the South China Sea (SCS) using the National Oceanic and Atmospheric Administration (NOAA) SST daily datasets for the period 1988–2009. In the SST over the South China Sea (SCS), a north-west versus south-east SST gradient (hereafter gra-SCS SST) is revealed. This SST gradient is seen to be induced by the distinct wind anomaly along with fresh water flux changes. The slope difference between the gra-SCS SST before and after 1999 is observed to be statistically significantly different than zero at a 95% confidence level. A decreasing/increasing trend in the gra-SCS SST is revealed before/after 1999. Besides, it is found that the gra-SCS SST characterizes the Asian monsoon variability by inducing cross equatorial monsoon flow towards the Asian Continent. In addition, we established the role of the gra-SCS SST in the Asian monsoon by computing causation based on the information flow concept between the gra-SCS SST and traditional monsoon indices, which pronounces that former impact the later. Based on the present corollary, we suggest that the gra-SCS SST should be considered as an important parameter in the climate studies as it is meticulously related to the precipitation over Asia.

Keywords : SST, South China Sea, monsoon, precipitation.

1. Introduction

The South China Sea (SCS) is one of the largest semi-enclosed marginal seas in the world ocean but the SCS remains poorly observed in terms of climate variability. It is connected with the East China Sea to the northeast, the Pacific Ocean and the Sulu Sea to the east, and the Java Sea and the Indian Ocean to the southwest. It is a very important region of interest for the scientific community because 1) the onset of the SCS summer monsoon (SM) indicates the onset of the East Asian SM [1], 2) Indian and East Asian monsoon systems exchange heat, momentum and moisture with the sea over the SCS [2], 3) the changes in Sea Surface Temperature (SST) over the SCS because of these fluxes during the monsoon affect chlorophyll concentration and therefore affects half billion people live along the coast of the SCS with its fisheries and other important resources [3], and 4) the anomalous state of the SCS can affect East and Southeast Asian climate [4] [5] [6] [7] hence have a profound influence on the social and economic condition of over 60% of the earth's population.

Moreover, the origin, development, and evolution of the SCS processes can greatly influence the weather and climate in East and Southeast Asia [8] [9], so it always necessary to comprehend the SST variability over the SCS. The SST over the SCS is considered as an important parameter in many operational and research activities, ranging from weather forecasting to climate research and plays a crucial role in maintaining the monsoon precipitation over the SCS and the surrounding area [7] [10]. Thus investigating the SST variability over the SCS region can help to figure out the influences of SCS

SST on rainfall. Moreover, it's worth to study SST s it is an important surface boundary conditions which are decisively important for the establishment of the monsoon circulation and rainfall [11] by modifying surface heat fluxes and the deep convection in the tropical atmosphere [12] [13] [14]. For example, in the recent study [14], the explicit prominence of SST (over the Bay of Bengal) in facilitates deep convection was remarkably identified. Besides, SST is considered to be the most important representative quantity of the ocean, which communicates the ocean's relatively large thermal inertia to the atmosphere, through an exchange of the surface fluxes [15] and indeed plays an important component in the precipitation variability. Therefore, in the view of the importance of the SST in the monsoon and because of the peculiar location of SCS where the most intense atmospheric convection associated with East Asia occurs, it is desirable to study the climate variability of SST over the SCS. The climate variability has become an important topic of scientific pursuit during the past few decades, intimately linking the economy of a nation with its climate-resources [16] [6] [17]. For example, [16] found that SST gradients across the equatorial Pacific undergo a regime change in 1998/99 due to a significant cooling (warming) over tropical eastern (western) Pacific in the later period. Recall that, SCS SST is largely influenced by one of the largest source of Earth's climate variability commonly known by El Niño–Southern Oscillation [18] [3] [19]. We intended to comprehend the climate variability of SST over the SCS and its association with Asian precipitation. To best of our knowledge, none of the previous studies so far brought out the SST gradient over the SCS, its associated oblivious trends and its association to Asian monsoon. In the following, first, list the data source and methodology, and then give a brief presentation of the results. This study is summarized in section 4.

2. Data and Methodology

The National Oceanic and Atmospheric Administration (NOAA) SST product from 1988 to 2009 (hereafter NOAA SST) based on the Advanced Very High-Resolution Radiometer (AVHRR) infrared observations merged with the Advanced Microwave Scanning Radiometer-Earth Observing System (AMSR E) is used (please refer to [20] [21] for more details) in the present study. Besides, National Center for Environmental Prediction (NCEP) - DOE AMIP 2 reanalysis daily datasets for wind fields [22], which are provided by the NOAA/OAR/ESRL PSD, Boulder, Colorado, USA, and are available from their website at http://www.esrl.noaa.gov/psd/ is also used for dynamical explanation. The precipitation data is taken from Asian Precipitation - Highly-Resolved Observational Data Integration Towards Evaluation (APHRODITE's) of Water Resources [23]. Surface salt flux observations are obtained from the Global Ocean Data Assimilation System (GODAS) developed at NCEP [24]. Notably, to obtain statistical significance, we followed two-tailed student t-test.

In methodologies, we will be using the traditional ones (e.g., regression analysis) and a newly developed tool for identifying the causality between time series. The causality from X_2 to X_1 (units: nats per unit time) is:

$$T_{2\to 1} = \frac{C_{11}C_{12}C_{2,d1} - C_{12}^2 C_{1,d1}}{C_{11}^2 C_{22} - C_{11}C_{12}^2}, \tag{1}$$

where C_{ij} is the sample covariance between X_i and X_j (i,j=1,2), and $C_{i,dj}$ the covariance between X_i and $[X_j(t+k\Delta t) - X_j(t)] / (k\Delta t)$, with Δt being the time step size and $k \geq 1$ some integer. Ideally, when $T_{2\to 1}$ is nonzero, then X_2 is causal to X_1, and vice versa (please refer [25] [26] for more details for computing causation).

Besides, to understand the underlying oceanography. we also computed the wind-driven vertical velocity at the bottom of Ekman layer using stress according to [27] and formulae is given below.
The vertical velocity at the bottom of the Ekman layer:

$$W_E = (1/\rho f)\,(curl_z \tau + \beta \tau_x / f) \tag{2}$$

here the Coriolis parameter f is equal to $2\Omega \sin \varphi$, where φ is the latitude, Ω is the rotation rate of Earth (7.29×10^{-5} rad s^{-1}), and β, the rate of change of the Carioles parameter with latitude, is equal to $2\Omega \cos \varphi / R$, with R equal to the radius of Earth (6.37×10^{6} m). $curl_z \tau$, the vertical component of wind stress curl, is defined by,

$$curl_z\tau = \partial\tau_y/\partial x - \partial\tau_x/\partial y \quad (3)$$

Wind stress and its components (τ , τ_x and τ_y) were computed using the bulk aerodynamic formulae. The meridional Ekman transport per unit zonal width computed as,

$$-\tau_x/\rho f \quad (4)$$

3. Results

The SST changes over SCS for the period 1988-1998 (PRE99) and 1999-2009 (POST99) is analyzed using the NOAA SST daily data sets. It is known that SCS SST is largely influenced by one of the largest sources of Earth's climate variability commonly known by El Niño–Southern Oscillation [1] [3] [19]. And since after the late 1990's, significant changes were seen over the Pacific Ocean due to the anomalous wind divergence in the central Pacific that cause a shift in the anomalous atmospheric convection westward, leading to a westward shift of the anomalous westerly response, thereby preventing the eastward propagation of the SST anomaly after the late 1990s [28]. For example, [28] and [16] found that the first leading empirical orthogonal function (EOF) mode of the POST99 tropical Pacific SSTA has shown maximum warming is the central Pacific (around 150°W), whereas the PRE99 EOF1 mode shows a warming in the eastern Pacific. So, therefore, it is of great scientific interest to comprehend the SST changes over the SCS during these two different periods; PRE99 and POST99. Analysis of the NOAA SST data reveals that mean SST during June, July, August, and September (hereafter JJAS) of PRE99 and POST99 is above 27°C (Figure 1a and 1b), which is conducive for enhanced convective precipitation [29] and is therefore of paramount importance.

Figure 1c represents JJAS SST differences, POST99 minus PRE99 which vividly shows that there exist substantial differences in the variability of SST during JJAS of PRE99 and POST99. It is found that these SST differences within the marked rectangular boxes in Figure 1(b) are statistically distinct from zero at a 99% level from that in 1(a). The shaded region in Figure 1d shows the statistical significant region. The substantial difference in SST is observed in the period PRE99 and POST99, particularly over regions 106°E; 115°E, 17°N; 22°N (hereafter region I) and 117°E; 120°E, 12°N; 17°N (hereafter region II) with the statistical significance of 99%. Interestingly, in the SST over SCS, a gradient in the SST with one center over north-west and another over south-east is found (Figure 1). To comprehend the SST gradient, the SST over region II is subtracted from that over region I, and we referred to it as gra-SCS SST.

The time series (solid line) and linear trends (dash line) of the gra-SCS JJAS SST from 1988 to 2009 are plotted in Figure 2. Clearly, we see that during POST99 the gra-SCS SST is significantly increased in comparison to PRE99. As seen from Figure 2, the gra-SCS SST has experienced a change in the pattern since PRE99. It is found that before 1999, the gra-SCS SST has a decreasing trend and whereas after 1999 the gra-SCS SST shows an increasing trend. Further, it is to be noted that the two slopes (gra-SCS SST for PRE99 and POST99) do not overlap and indeed observed to be statistical significance at a 95% confidence level. Essentially, we find that, at a 95% confidence level, the two slopes are -3.64 ± 1.03 and 0.63 ± 1.00 (both are multiplied by 10E-4) respectively and they lie within a confidence interval of [-4.65, -2.61] and [-0.37, 1.63]. And these do not overlap because it is clearly evident from the interval that during PRE99 the interval is ending at -2.61 and while during the POST99 interval is starting from -0.37, thus we can say that the two slopes indeed completely differ at a 95% confidence level. The least squares method applied to estimate the slope is already being used in our recent study [14]. This distinguishes the role of the gra-SCS SST during the two different climate phases PRE99 and POST99.

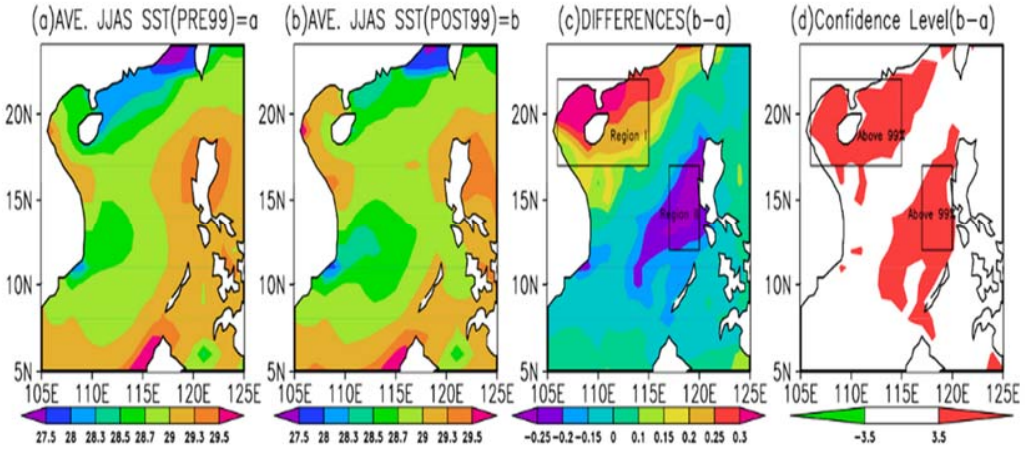

Figure 1. Average JJAS SST gra-SCS (in ^{o}C) (a) PRE99 (b) POST99 (c) POST99 minus PRE99 and (d) represent (b) is statistically distinct from zero at a 99% level from that in (a).

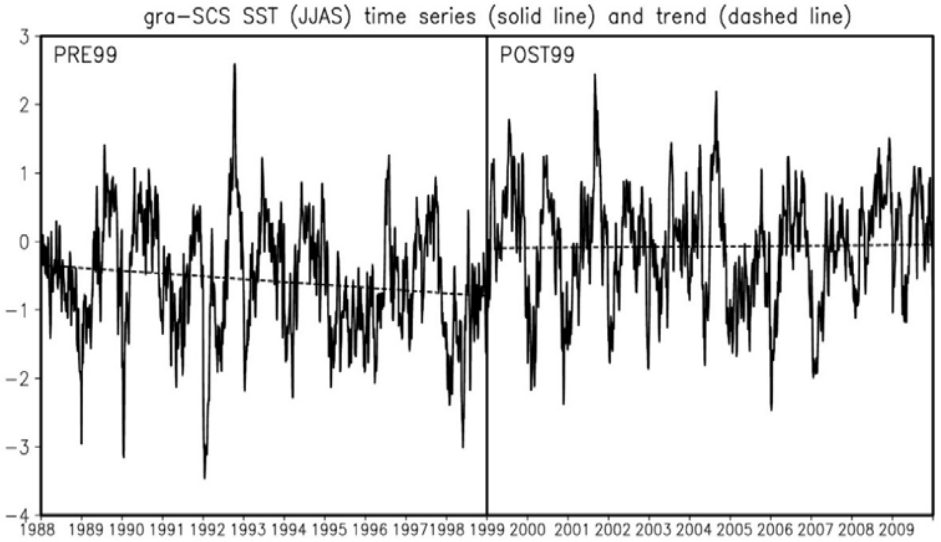

Figure 2. gra-SCS SST (JJAS) time series (solid line) and trend (dashed line). The trend plotted is statistically significant at 99% confidence level.

In the next, the possible dynamical reason behind the gra-SCS SST change during the study period is explored. It is identified that the gra-SCS SST variation during the POST99 seems to be associated with the distinctive wind patterns (Figure 3a). The distinctive wind pattern is clearly seen over the gra-SCS SST region. The decreased/increased wind speed (Figure 3a) along with the presence of high/low freshwater influx (Figure 3b) is observed during POST99. And, this seems to be the cause of SST increase/decrease during POST99 over the region I/region II respectively. Because it is well known that the presence freshwater in flux and low-intensity winds can break down the stable stratification that forms due to the flux and results in leaving the ocean warmer than most of the other parts of the Ocean,

this is indeed natural and known fact [30]. Apart from this, an attempt has also been made to understand the underlying oceanography and hence vertical velocity at the bottom of Ekman layer and meridional Ekman transport per unit zonal width along 17°N during POST99 minus PRE99 also been computed (Figure 3c and Figure 3d). A clear contribution of Ekman transport to coastal upwelling is depicted from the analysis. It reveals that another possible reason to the reduction of SST over the region II is the coastal upwelling along with the maximum positive (or northward) Ekman transport (which can be seen between 116°E and 122°E).

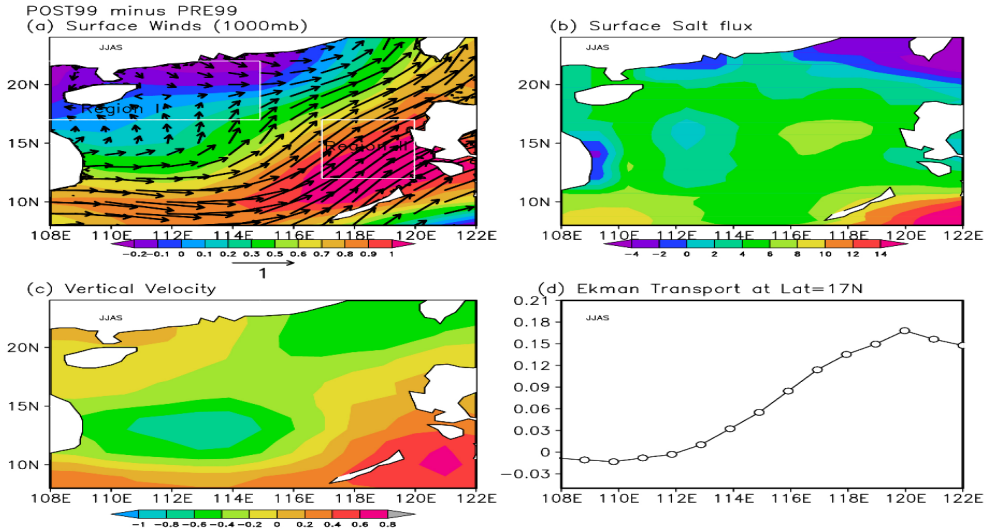

Figure 3. POST99 minus PRE99 differences during JJAS (a) surface (1000hpa level) wind magnitude/vector difference represent by shaded/arrow (b) surface salt flux (in x10^{-8}g/cm^2/s) (c) vertical velocity at the bottom of Ekman layer (in x 10^{-6} m/s) (d) meridional Ekman transport per unit zonal width along 17°N.

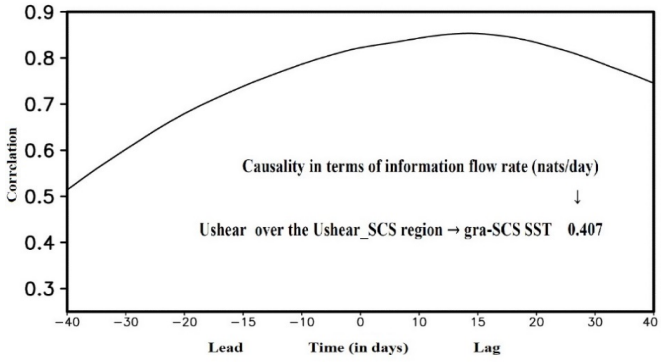

Figure 4. Lead-lag correlation between the gra-SCS SST and the Ushear over the Ushear_SCS region; a positive number means that the gra-SCS SST lags Ushear over the Ushear_SCS region (in days). The correlation coefficient is statistically significant at 99% confidence level.

Moreover, in order to strengthen our claim, especially the role of wind fields in the gra-SCS SST, the association of wind fields with gra-SCS SST is further explored by computing the lead-lad correlation followed by examining the causation in a quantitative way (please refer [25] [26] for more details for computing causation) between the gra-SCS SST and the U shear (U850-U200) over the SCS region (105°;120°E, 5°-20°N; hereafter called as Ushear_SCS region). It is to be noted that the Ushear region chosen here is similar to Liang et al., (2002) and it is of crucial importance in terms of SCS, as it characterizes the broad-scale feature of the SCS [31]. The results reveal a significantly high correlation

between the Ushear_SCS region and gra-SCS SST (Figure 4). Further correlation analysis reveals the possible contribution of Ushear_SCS (Ushear_SCS seems to lead the gra-SCS SST) to gra-SCS SST. To corroborate the findings, information flow rates from the Ushear_SCS region to gra-SCS SST is computed and it is found to be 0.407 nats/day at 95% significant level. This indeed says that there is causation from Ushear_SCS region to gra-SCS SST. Thus, in other words, we can say that the former could be one of the causes for the latter and this is in accordance with aforementioned findings.

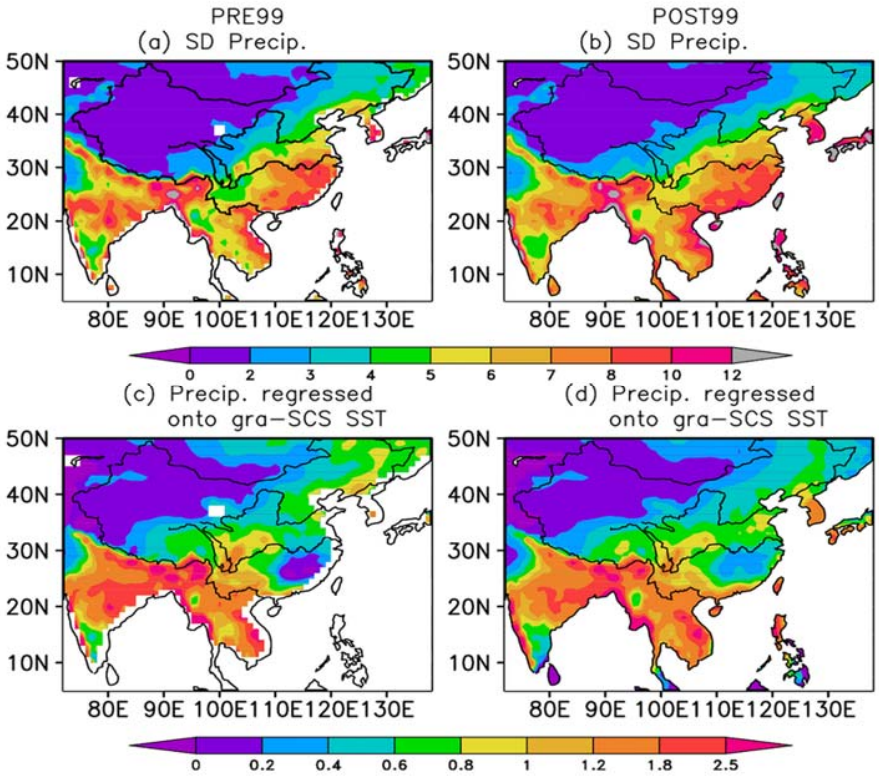

Figure 5. (a) and (b) are the standard deviation of the precipitation, (c) and (d) are precipitation regressed onto the gra-SCS SST for PRE99 (left panel) and POST99 (right panel). The regression coefficient is statistically significant at 99% confidence level.

Seeing at the SCS SST potent and knowledge which states that Asian monsoon system (which includes the South Asian monsoon and the East Asian monsoon) begins over the SCS [18], it is highly recommended to talk over the relationship between the SCS SST gradient and precipitation over the Asian region. Therefore, we analyzed the precipitation variability and its association with the SCS gradient in SST (Figure 5). To do so, we regressed the precipitation onto the gra-SCS SST for PRE99 (Figure 5c) and POST99 (Figure 5d) using the least square regression method. The regression equation has the form Y=a+bX, where X and Y are two variables, *b* is the slope of the line, and *a* is the y-intercept. In this case, X is the gra-SCS SST time series and Y the series of gridded precipitation values on a 1° x 1° latitude-longitude grid. Both the series have a time resolution of 1 day, and the regressed precipitation is plotted in Figure 5c (during PRE99) and 5d (during POST99). Interestingly, the comparison between Figure 5 (a and c) and Figure 5(b and d) shows that the precipitation variability over the vast region of East and South Asia can be well explained by the gra-SCS SST. Besides, we also have drawn the differences (POST99 minus PRE99) in standard deviation in precipitation and regressed values of

precipitation in Figure 6. If we compare Figure 6a and Figure 6b, the similarity can be clearly evident. In other words, the analysis reveals that gra-SCS SST bears a strong relationship with the precipitation variability over Asia. Thus, we may say that gra-SCS SST must be considered as an important parameter in the climate studies as it is closely related to precipitation over Asia.

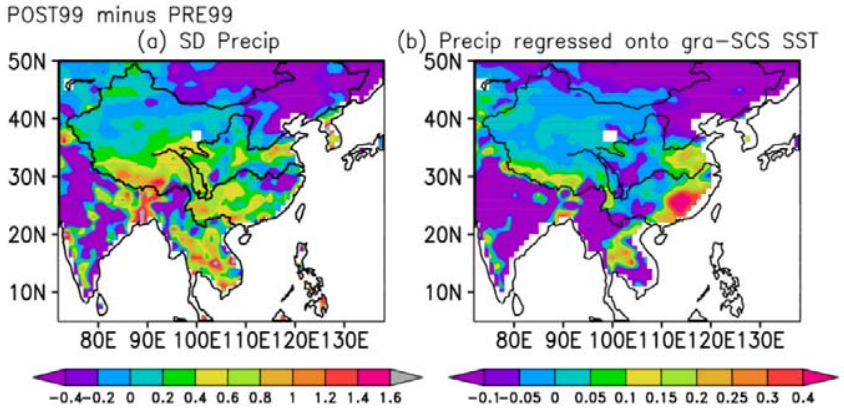

Figure 6. (a) alike Figure 5a but for POST99 minus PRE99 differences, and (b) alike Figure 5c but for POST99 minus PRE99 differences.

Since it is evident, that wind shear is the deep-rooted component that drives the monsoon precipitation over Asia [32] [33]. So to describe the gra-SCS SST association with precipitation over Asia, the wind shear over the Asian region is examined. To investigate this, we regressed the wind shear over the Asian region onto gra-SCS SST (Figure 7). It is clearly evident that gra-SCS SST induces a cross-equatorial shear flow towards the Asian Continent in order to participate actively in the dynamics of Asian monsoon (Figure 7c and 7f). Further, to make corroboration on the role of gra-SCS SST in the Asian monsoon, we examine the causation (by applying aforementioned discussed rigorously causality analysis) between the gra-SCS SST and traditional monsoon indices which are used to define Asian monsoon in a quantitative way. The tradition monsoon indices on which causation has been applied are Webster and Yang circulation index (hereafter USHEAR index) and Goswami monsoon Hadley circulation index (hereafter VSHEAR index); please refer [32] and [33] respectively for more details regarding tradition monsoon indices. The USHEAR index is defined as a time-mean zonal wind (U) shear between 850 hPa and 200 hPa, written U850 − U200, averaged over South Asia from the equator to 20°N and from 40° to 110°E (region is marked in Figure 7d) and the VSHEAR index is defined by the meridional wind (V) shear between 850 hPa and 200 hPa (V850–V200) averaged over the region 70°; 110°E, 10°; 30°N (region is marked in Figure 7e). We found a significant (at 95% level) causation between 1) gra-SCS SST and USHEAR index and 2) gra-SCS SST and VSHEAR index. In case (1), the flow rate is 0.242 nats/day. In case of (2), the flow rate is 0.144 nats/day. The significant causation between the gra-SCS SST and the monsoon index (USHEAR and VSHEAR) is found, i.e., we can say that the former could be one of the causes for the latter, which is indeed overwhelming because this reveals the interaction of SCS SST with Asian monsoon quantitatively. Also drawn are the POST99 minus PRE99 differences of the regressed U shear, V shear and UV shear vectors (Figure 8). Interestingly, an unambiguous role of the gra-SCS can be depicted in the differences as shown in Figure 8c. It shows a precise association between the gra-SCS and weakening of the cross-equatorial flow in the recent decade. The weakening of cross-equatorial monsoon flow and its association to the Indian Ocean is already been reported in the recent study [34]. Nevertheless, the exact cause of the weakening of large-scale cross-equatorial monsoon flow is still an open debate for the scientific community. Based on Figure 8 findings, we suggest that the gra-SCS is one of the reasons for the weakening of the large-

scale cross-equatorial monsoon flow in the recent decade. However, we keep it as debatable until a detailed study using an adequate model with the gra-SCS SST forcing data is done because we feel that it would be necessary before a conclusive statement can be made. We leave this concern for future study.

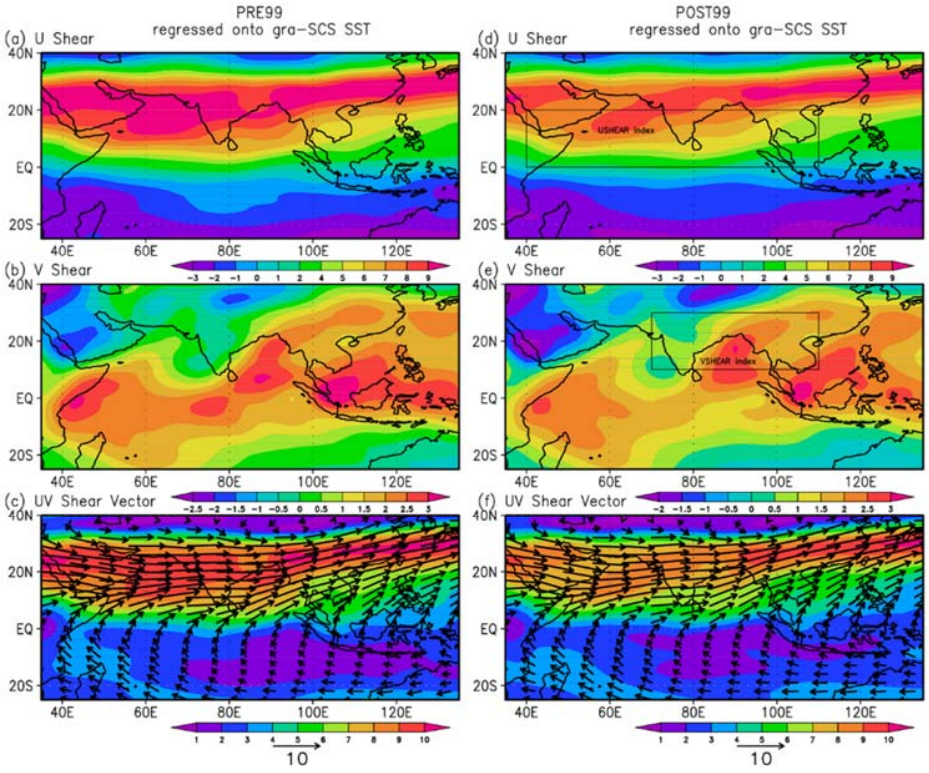

Figure 7. (a) and (d) are U shear regressed onto gra-SCS SST, (b) and (e) are V shear regressed onto gra-SCS SST, (c) and (f) are UV shear regressed onto gra-SCS SST for PRE99 (left panel) and POST99 (right panel). The regression coefficient is statistically significant at 99% confidence level.

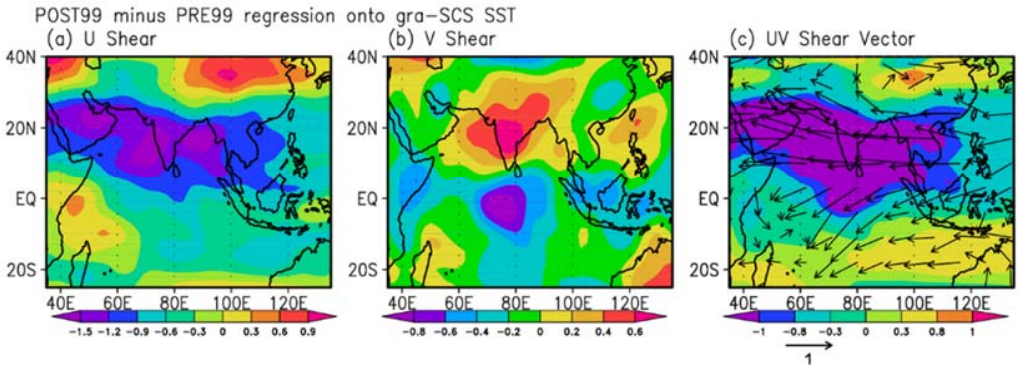

Figure 8. (a) alike Figure 7a but for POST99 minus PRE99 differences, (b) alike Figure 7b but for POST99 minus PRE99 differences, and (c) alike Figure 7c but for POST99 minus PRE99 differences.

4. Summary

Our analysis with the daily mean NOAA SST data has shown the gra-SCS SST has distinctly different climatic patterns before and after 1999, which is referred to as PRE99 and POST99 respectively. In the SST over the SCS, a north-west versus south-east SST gradient is revealed. The gra-SCS SST is identified to have decreasing slope before 1999 and increasing since 1999. This gra-SCS SST is seen to induced by the distinct wind anomaly along with fresh water flux changes and underlying oceanic processes. Interestingly, it is found that gra-SCS SST shares a strong relationship with precipitation over Asia by inducing the cross-equatorial monsoon shear flow towards the Asian Continent. Further corroboration made on the role of gra-SCS SST in the Asian monsoon by using established information flow concept between gra-SCS SST and traditional monsoon indices. It reveals explicit causation between gra-SCS SST to the monsoon indices. Thus with all due fairness, the present study proposed that the gra-SCS SST must be considered as important in climate change signals in describing the precipitation variability over Asia.

Acknowledgments

The comment from an anonymous referee is appreciated. The author thanks NOAA High-Resolution SST, NCEP-DOE AMIP 2 reanalysis and the APHRODITE's team for providing the data and ICTMAS's organizing committee for generous support. The Key Laboratory of Meteorological Disaster of Ministry of Education (KLME1603) and the Jiangsu Provincial Government through the 2015 Jiangsu Program for Innovation Research and Entrepreneurship Groups for the financial support. The figures were prepared using GrADS.

5. References

[1] Wang B and Lin H 2002 Rainy season of the Asian-Pacific summer monsoon *J. Clim*. **15** 386–396
[2] Mao J Y and Chan J C L 2005 Intraseasonal variability of the SCS SM *J. Clim.* **18(13)** 2388–2402
[3] Xie S P, Xie Q, Wang D and Liu W T 2003 Summer upwelling in the South China Sea and its role in regional climate variations *J. Geophys. Res.* **108(C8)** 3261. doi:10.1029/2003JC001867
[4] Zhou L, Tam CY, Zhou W and Chan J C L 2010 Influence of SCS SST and the ENSO on winter rainfall over South China *Adv. Atmos. Sci.* **27** 832-844. doi: 10.1007/s00376-009-9102-7
[5] Roxy M and Tanimoto Y 2011 Influence of SST on the intraseasonal variability of the South China Sea Summer Monsoon *Clim. Dyn.* **39 (5)** 1209 – 1218. DOI: 10.1007/s00382 – 011 – 1118 – x
[6] Vaid B H and Polito P S 2016 Influence of the SCS biweekly SST on SCS SM especially during Indian Ocean Dipole *Atmosphere-Ocean* **54(1)** 48-59 DOI:10.1080/07055900.2015.1130682
[7] Vaid B H 2017 Biweekly SST over the SCS and its association with the Western North Pacific SM Pure *Appl. Geophys.* **174** 463–475. DOI: 10.1007/s00024-015-1198-3
[8] Scsmex Project Office 1995 Scientific Plan of the South China Sea Monsoon Experiment (SCSMEX) Published by SCSMEX Project Office pp 42
[9] Ding Y H 2004 Seasonal march of the East Asian summer monsoon In*: The East Asian Monsoon* (Chang CP, ed). Singapore. World Scientific Publisher pp 560
[10] Vaid B H, Preethi B and Kripalani R H 2018 The Asymmetric Influence of the South China Sea Biweekly SST on the Abnormal Indian Monsoon Rainfall of 2002 *Pure Appl. Geophys.* 175(12) 4625–4642. doi.org/10.1007/s00024-018-1934-6
[11] Webster P J, Magana V O, Palmer T N, Shukla J, Tomas RA, Yanai M and Yasunari T 1998 Monsoons: process, predictability and the prospects for prediction *J. Geophys. Res.* **103(C7)** 14451–14510
[12] Thum N, Esbensen S K, Chelton D B and Mcphaden M J 2002 Air-sea heat exchange across the northern equatorial SST front in the eastern tropical Pacific *J. Clim.* **15** 3361–3378
[13] Raymond D J, Esbensen S K, Paulson C, Gregg M, Bretherton C S, Petersen W A, Cifelli R, Shay L K, Ohlmann C, and Zuidema P 2004 EPIC2001 and the coupled ocean-atmosphere system of the tropical east Pacific *Bull. Am. Meteorol. Soc.* **85** 1341–1354
[14] Vaid B H and Liang X S 2018a The changing relationship between the convection over the western Tibetan Plateau and the sea surface temperature in the northern Bay of Bengal *Tellus A: Dynamic Meteorology and Oceanography* **70**(1) 1440869
[15] Deser C, Alexander M A, Xie SP and Phillips A S 2010 Sea surface temperature variability: patterns and mechanisms *Ann. Rev. Mar. Sci.* **2** 115–143

[16] Chung P H and Li T 2013 Interdecadal relationship between the mean state and El Nino types *J. Clim.* **26** (2) 361-379
[17] Vaid B H and Liang X S 2018b An Abrupt Change in Tropospheric Temperature Gradient and Moisture Transport Over East Asia in the Late 1990s *Atmosphere-Ocean* DOI: 10.1080/07055900.2018.1429381
[18] Wang Q, Liu Q, Hu R and Xie Q 2002 A possible role of the South China Sea in ENSO cycle *Acta Oceanol. Sin.* **21** 217–226
[19] Wang C, Wang W, Wang D and Wang Q 2006 Interannual variability of the South China Sea associated with El Niño *J. Geophys. Res***. 111** C03023. doi:10.1029/2005JC003333
[20] Reynolds RW, Smith T M, Liu C, Chelton D B, Casey K S and Schlax M G 2007 Daily high-resolution blended analyses for sea surface temperature *J. Clim.* **20** 5473-5496
[21] Vaid B H, Gnanaseelan C, and Kumar J 2011 Intraseasonal oscillation in Reynold SST over the tropical Indian Ocean and their validation *Int. J. Rem. Sens.* 09/2011, **32(17-17**) 4835-4856. DOI:10.1080/01431161.2010.489585
[22] Kanamitsu M, Ebisuzaki W, Woollen J, Yang S K, Hnilo J, Fiorino M and Potter G L 2002 NCEP-DOE AMIP-II Reanalysis (R-2) *Bull. Am. Meteorol. Soc.* **83** 1631-1643
[23] Yatagai AK, Kamiguchi A O, Hamada A, Yasutomi N and Kitoh A 2012 APHRODITE: Constructing a Long-term Daily Gridded Precipitation dataset for Asia based on a Dense Network of Rain Gauges *Bulletin of American Meteorological Society* **93(9)** 1401-1415 doi:10.1175/BAMS-D-11-00122.1
[24] Saha S, et al. 2006 The NCEP climate forecast system *J Clim.* **19** 3483–3517
[25] Liang X S 2014 Unraveling the cause-effect relation between time series *Phys. Rev. E.* **90**:052150
[26] Liang X S 2016 Information flow and causality as rigorous notions ab initio *Phys. Rev. E*. **94** 52201
[27] Stommel H M 1965 *The Gulf Stream Berkeley*: University of California Press. pp 248
[28] Xiang B, Wang B and Li T 2013 A new paradigm for the predominance of standing Central Pacific Warming after the late 1990s *Clim. Dyn.* **41** (2) 327-340
[29] Lau KM, Wu H T and Bony S 1997 The role of large-scale atmospheric circulation in the relationship between tropical convection and sea surface temperature *J. Clim.* **10**(3) 381–392
[30] Shenoi S S C, Shankar D and Shetye S R 2002 Differences in heat budgets of the near-surface Arabian Sea and BOB: implications for the summer monsoon *J. Geophys. Res.* **107** 1-14. doi:10.1029/2000JC000679
[31] Liang J and Shang-Sen W U 2002 A Study of Southwest Monsoon onset date over the South China Sea and its impact factors Chin *J. Atmos. Sci*. **26**(6) 829-844
[32] Webster P J and Yang S 1992 Monsoon and ENSO: Selectively interactive systems *Quart. J. Roy. Meteor. Soc.* **118** 877–926
[33] Goswami B N, Krishnamurthy V and Annamalai H 1999 A broad scale circulation index for interannual variability of the Indian summer monsoon *Quart. J. Roy. Meteor. Soc.* **125** 611–633
[34] Swapna P, Krishnan R and Wallace J M 2014 Indian Ocean and monsoon coupled interactions in a warming environment *Clim. Dyn.* **42** 2439–2454